Nonlinear optical rectification of GaAs/$Ga_{1-x}Al_xAs$ quantum dots with Hulthén plus Hellmann confining potential

Yi-Ming Duan(段一名) and Xue-Chao Li(李学超)†

School of Mechanics and Optoelectronics Physics, Anhui University of Science and Technology, Huainan 232001, *China*

(Received 8 April 2022; revised manuscript received 12 May 2022; accepted manuscript online 18 May 2022)

We investigate the nonlinear optical rectification (NOR) of spherical quantum dots (QDs) under Hulthén plus Hellmann confining potential with the external tuning elements. Energy and wavefunction are determined by using the Nikiforov–Uvarov method. Expression for the NOR coefficient is derived by the density matrix theory. The results show that the applied external elements and internal parameters of this system have a strong influence on intraband nonlinear optical properties. It is hopeful that this tuning of the nonlinear optical properties of GaAs/$Ga_{1-x}Al_xAs$ QDs can make a greater contribution to preparation of new functional optical devices.

Keywords: nonlinear optical rectification, quantum dots, Hulthén plus Hellmann potential, Nikiforov–Uvarov method

PACS: 73.21.La, 96.12.Hg, 33.80.–b **DOI:** 10.1088/1674-1056/ac70bf

1. Introduction

Generation of laser can provide powerful conditions for uncovering the veil of nonlinear optics. High intensity and strong coherence are the characteristics of laser beams.[1–4] Moreover, generation of nonlinear optical effects requires beams with these characteristics to react with materials. When the laser was born, the theory of nonlinear optics also entered a rapid writing stage.[5,6] After that, scientists interact different laser beams with different media, and constantly find new nonlinear optical phenomena, such as optical sum frequency, optical rectification, third harmonic, and frequency doubling.[7–9] In the past ten years, new nonlinear optical effects were found, and furthermore scientists have paid more attention to development of nonlinear optical devices. For example, optical parametric oscillators are made by using three wave mixing in nonlinear optical effect. Light modulators can modulate phase and intensity of emitted light.[10,11] These optical devices mainly use the second-order and third-order nonlinear optical effects. In addition, nonlinear optical effects also have important applications in the field of information communication.

The appearance of semiconductor nano materials plays an important role in generation of new nonlinear optical phenomena. Due to the size effect of electrons in semiconductor nano materials, the changes of energy level and energy state will also be greatly affected in the process of interaction with light field.[12–14] Quantum dots (QDs) are particles composed of several atoms with a diameter of about 1–10 nm. QDs are generally presented in core-shell structure, and their cores can be composed of metal complexes such as CdSe and ZnO. The "shell" can be composed of metal complexes such as ZnS, which shields the core and forms an electrostatic potential with the core.[15–17] The physical properties of quantum dots are similar to those of basic atoms, but they are more "flexible" than atoms. It can enclose single or multiple electrons in a small space, so that the electrons are limited in the three-dimensional direction, which will make the quantum confinement effect and size effect more significant than other semiconductor materials such as quantum wires or quantum wells.[18–20] Recently, numerous research have focused on nonlinear optical properties of QDs. For instance, Prasad *et al.*[21] reported optical properties of disk shaped QDs with magnetic fields. Rezaei *et al.*[22] examined the nonlinear optical properties on an ellipsoidal finite potential QDs. Liu *et al.*[23] studied nonlinear optical properties of disk-shaped QDs under a static magnetic field. Hou *et al.*[24] investigated third-order nonlinear optical properties on black phosphorus QDs. Liu *et al.*[25] analyzed the nonlinear optical properties on the composite films with CdSe QDs. This paper mainly discusses the nonlinear optical rectification (NOR) of GaAs/$Ga_{1-x}Al_xAs$ QDs under Hulthén-plus-Hellmann (HPH) potential, which is influenced by external factors, for instance, Al-concentration and temperature. This research may provide new ideas and new methods for manufacture of new optical devices.

Our article is structured as follows: The bound state solutions of the Schrödinger equation are given with the Nikiforov–Uvarov (NU) method in Section 2. Then, the expression of the NOR coefficient is provided. In Section 2, we present the results of GaAs/$Ga_{1-x}Al_xAs$ spherical quantum dots and discussions. Finally, in Section 4 we show a summary of the obtained results.

†Corresponding author. E-mail: xuechao80@126.com

© 2023 Chinese Physical Society and IOP Publishing Ltd

2. Model and analysis

The radial Schrödinger equation for a confined electron utilizes the effective mass approximation given by

$$\frac{\mathrm{d}^2\psi_{nl}(r)}{\mathrm{d}r^2}+\frac{2m^*(x,P,T)}{\hbar^2}\times\left[E_{nl}-V(r)-\frac{\hbar^2 l(l+1)}{2m^*(x,P,T)}\frac{1}{r^2}\right]\psi_{nl}(r)=0, \quad (1)$$

where $V(r)$ means the limiting potential, $m^*(x,P,T)$ means the effective mass of electrons of GaAs/$Ga_{1-x}Al_xAs$ materials affected by x, P, T.[26,27] In our paper, we take $V(r)$ as the HPH potential:[28–30]

$$V(r)=-\frac{V_1\,\mathrm{e}^{-\alpha r}}{1-\mathrm{e}^{-\alpha r}}-\frac{A}{r}+\frac{B\mathrm{e}^{-\alpha r}}{r}, \quad (2)$$

where α means the adjustable screening parameter, $A=V_2R_0$, $B=V_3R_0$, α is a parameter related to the dot radius. V_1 means the depth of Hulthén potential, V_2 and V_3 represent the strengths of Coulomb and Yukawa confining potentials, respectively. To solve Eq. (1), we use the following Greene–Aldrich approximation:[31]

$$\frac{1}{r^2}\approx\frac{\alpha^2}{(1-\mathrm{e}^{-\alpha r})^2}. \quad (3)$$

Combining Eqs. (1)– (3) yields

$$\frac{\mathrm{d}^2\psi_{nl}(r)}{\mathrm{d}r^2}+\frac{2m^*(x,P,T)}{\hbar^2}\times\left[E_{nl}+\frac{V_1\,\mathrm{e}^{-\alpha r}}{1-\mathrm{e}^{-\alpha r}}+\frac{A\alpha}{1-\mathrm{e}^{-\alpha r}}-\frac{B\alpha\,\mathrm{e}^{-\alpha r}}{1-\mathrm{e}^{-\alpha r}}-\frac{\hbar^2 l(l+1)}{2m^*(x,P,T)}\frac{\alpha^2}{(1-\mathrm{e}^{-\alpha r})^2}\right]\psi_{nl}(r)=0. \quad (4)$$

New coordinates will be introduced using the variable $r\to s$:

$$s=\mathrm{e}^{-\alpha r}. \quad (5)$$

Then

$$\frac{\mathrm{d}^2\psi(s)}{\mathrm{d}s^2}+\frac{1}{s}\frac{\mathrm{d}\psi(s)}{\mathrm{d}s}+\frac{1}{s^2(1-s)^2}\times\left[-(\varsigma+k_1-k_3)s^2+(2\varsigma+k_1-k_2-k_3)s-(\varsigma-k_2+k_4)\right]\psi(s)=0, \quad (6)$$

where

$$-\varsigma=\frac{2m^*(x,P,T)E_{nl}}{\hbar^2\alpha^2},\quad k_1=\frac{2m^*(x,P,T)V_1}{\hbar^2\alpha^2},\quad k_2=\frac{2m^*(x,P,T)A}{\hbar^2\alpha},\quad k_3=\frac{2m^*(x,P,T)B}{\hbar^2\alpha},\quad k_4=l(l+1). \quad (7)$$

Finally, we obtain the expression of energy eigenvalues of HPH confining potential as follows:

$$E_{nl}=\frac{\hbar^2\alpha^2 l(l+1)}{2m^*(x,P,T)}-A\alpha-\frac{\hbar^2\alpha^2}{8m^*(x,P,T)}\times\left[\frac{(n+l+1)^2+k_3-k_2-k_1+l(l+1)}{(n+l+1)}\right]^2. \quad (8)$$

Similarly, we obtain

$$\psi_{nl}(s)=N_{nl}s^{\sqrt{\omega_3}}(1-s)^{(0.5+\sqrt{\omega_3+\omega_2+\omega_1})}\times P_n^{(2\sqrt{\omega_3},2\sqrt{\omega_3+\omega_2+\omega_1})}(1-2s). \quad (9)$$

where

$$\omega_1=\frac{1}{4}+\varsigma+k_1-k_3,\quad \omega_2=2\varsigma+k_1-k_2-k_3,\quad \omega_3=\varsigma-k_2+k_4. \quad (10)$$

In our work, the expression of the NOR coefficient is given as[32,33]

$$\chi_0^{(2)}=\frac{4\mathrm{e}^3\sigma_v}{\varepsilon_0\hbar^2}M_{01}^2\delta_{01}\frac{\omega_{10}^2\left(1+\frac{\Gamma_2}{\Gamma_1}\right)+(\omega^2+\Gamma_2^2)\left(\frac{\Gamma_2}{\Gamma_1}-1\right)}{\left[(\omega-\omega_{10})^2+\Gamma_2^2\right]\left[(\omega+\omega_{10})^2+\Gamma_2^2\right]}, \quad (11)$$

where σ_v denotes the electron density, $M_{ij}=|\langle\Psi_j|r\cos\theta|\Psi_i\rangle|$ denotes the matrix element, $\delta_{01}=|M_{11}-M_{00}|$, $\omega_{ij}=(E_i-E_j)/\hbar$ denotes the transition frequency.

3. Results and discussions

In this section, the NOR coefficient in QDs with the HPH potential is explored. The parameters used in the calculations are taken as[32,33] $\sigma_v=5\times10^{24}\ \mathrm{m}^{-3}$, $T_1=0.2$ ps, $T_2=0.14$ ps, $\Gamma_1=1/T_1$, $\Gamma_2=1/T_2$, $\varepsilon_0=8.85\times10^{-12}\ \mathrm{F\cdot m}^{-1}$.

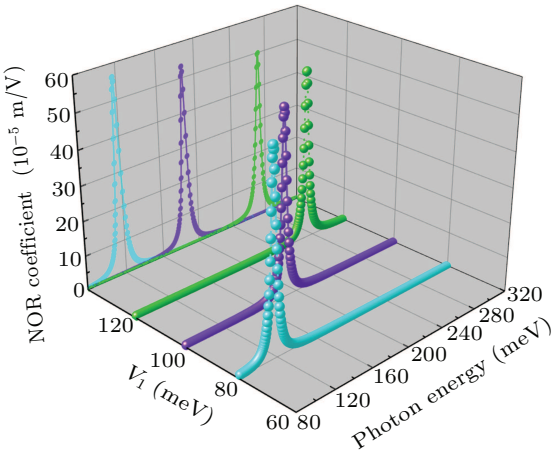


Fig. 1. NOR coefficient susceptibility with photon energies for $x=0.2$, $P=12$ kbar, $T=300$ K, $R_0=5$ nm, $V_2=100$ meV, $V_3=100$ meV as various values of V_1.

Figure 1 shows the behavior of the NOR coefficient for different situations of the depth V_1, take the fixed values of $x=0.2$, $P=12$ kbar, $T=300$ K, $R_0=5$ nm, $V_2=100$ meV, and $V_3=100$ meV. We can find that as the value of V_1 increases i.e., the limit increases, the energy difference E_{10} increases, corresponding to the NOR coefficient peak moving towards the larger value of the photon energy direction, and

the peak appears blue shift. Moreover, the increase of V_1 will lead to the decrease of $M_{01}^2\delta_{01}$ when the depth is changed from 80 meV to 120 meV. As seen in curves, when the depth value is 80 meV, the maximum of the NOR coefficient can reach 56.27×10^{-5} m/V. When the depth increases to 100 meV, the maximum decreases distinctly to 53.16×10^{-5} m/V. However, when the depth increases to 120 meV, the maximum decreases slightly to 49.85×10^{-5} m/V.

As shown in Fig. 2, the variation of the NOR coefficient with R_0 is displayed by taking $V_0 = 100$ meV, $x = 0.2$, $P = 12$ kbar, $T = 300$ K, $V_2 = 100$ meV, and $V_3 = 100$ meV. We can obtain that the NOR coefficient shifts toward high energy direction with the strengthening of R_0. The physical reason is that, when the R_0 is within the limit, E_{10} increases with increment. Specifically, the resonant peak of NOR coefficient increases as R_0 increases, which is owing to an increment in the matrix element $M_{01}^2\delta_{01}$.

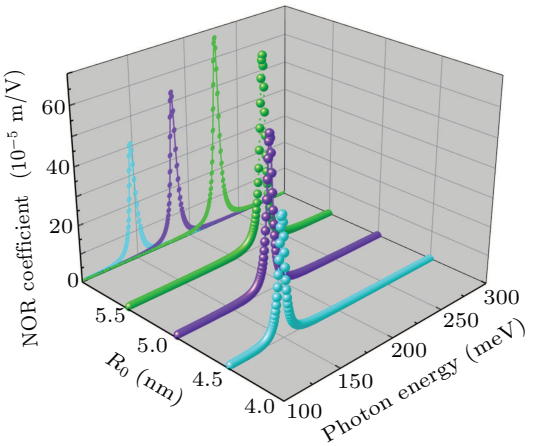


Fig. 2. NOR coefficient susceptibility with photon energies for $V_1 = 100$ meV, $x = 0.2$, $P = 12$ kbar, $T = 300$ K, $V_2 = 100$ meV, and $V_3 = 100$ meV with different values of R_0.

Figure 3 presents a functional diagram for different Al-concentration x on the NOR coefficient with other parameters being fixed. As seen in curves, it is clear that in the increasing process of Al-concentration from 0.1 to 0.3, the peak value slightly decreases with an increment of Al-concentration. We find that, when x is 0.1, the value of the $M_{01}^2\delta_{01}$ is 6.49×10^{-27} m^3; when x increases to 0.2, the $M_{01}^2\delta_{01}$ becomes 6.37×10^{-27} m^3; when x changes to 0.3, the value of the density matrix increases to 6.28×10^{-27} m^3. Specifically, with increasing x, the location of NOR coefficient shifts blue, which results from the increasing E_{10}.

Figure 4 shows the effects of (a) hydrostatic pressure P and (b) temperature T on the NOR coefficients for $x = 0.2$, $V_1 = 100$ meV, $V_2 = 100$ meV, $V_3 = 100$ meV, and $R_0 = 5$ nm. From Fig. 4(a), as the P increases, the NOR coefficient moves towards the high energy region, i.e., blue shift. Moreover, the increase of P reduces the size of the matrix element, which is owing to the P that has the effect of reducing constraints. In Fig. 4(b), there is a red shift with increasing T and the NOR coefficient peak increases with increasing T, because the separation between energies decreases.

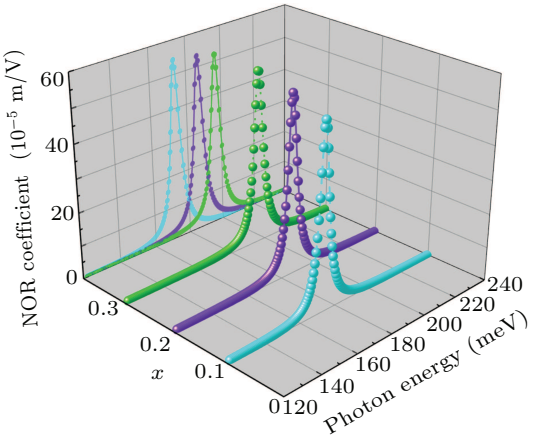


Fig. 3. NOR coefficient susceptibility with photon energies with $R_0 = 5$ nm, $P = 12$ kbar, $T = 300$ K, $V_1 = 100$ meV, $V_2 = 100$ meV, and $V_3 = 100$ meV for different x.

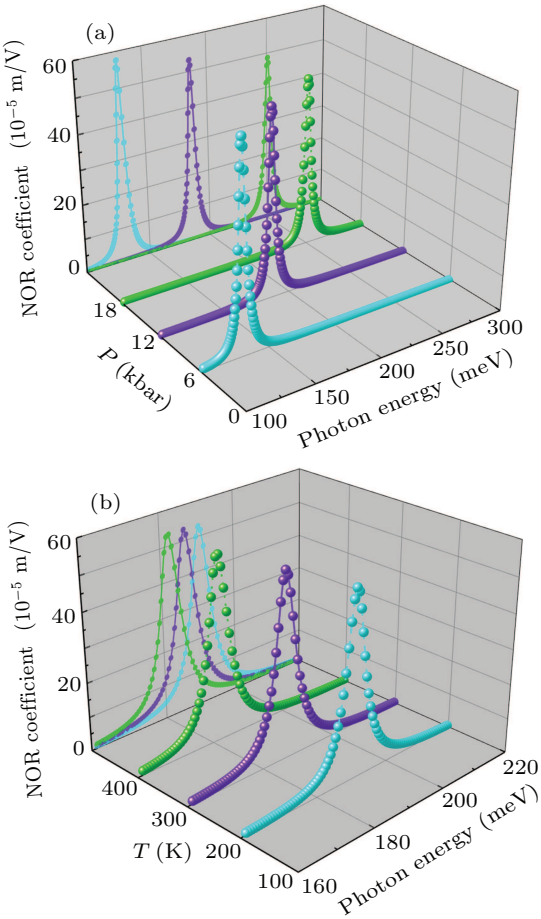


Fig. 4. NOR coefficient susceptibility with photon energies with $x = 0.2$, $V_1 = 100$ meV, $V_2 = 100$ meV, $V_3 = 100$ meV, and $R_0 = 5$ nm for different P (a) and T (b).

Figure 5 shows the coefficients of NOR for the potential strengths V_2 (a) and V_3 (b) against $\hbar\omega$. We can conclude that the NOR coefficient peak blue shifts when V_2 is reduced to 80 meV from 120 meV. Also, increasing V_2 results in a decrement in the peak amplitude. However, the increment of V_3 in Fig. 5(b) on the coefficient leads to an apparent redshift of

the NOR coefficient peak and leads to an increase in the NOR coefficient.

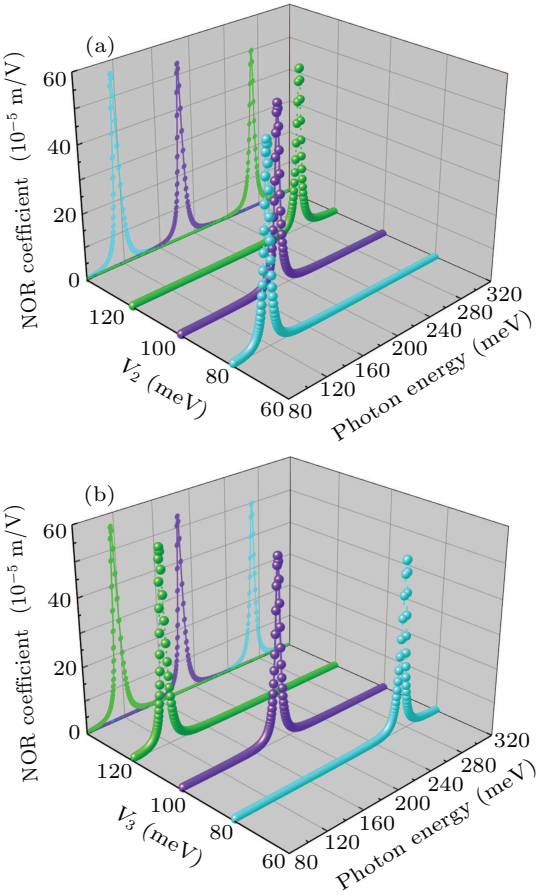


Fig. 5. NOR coefficient susceptibility with photon energies with $R_0 =$ 5 nm, $x = 0.2$, $V_1 = 100$ meV, $P = 12$ kbar, and $T = 300$ K for different V_2 (a) and V_3 (b).

4. Conclusion

In summary, we have derived the expressions of wave function and energy eigenvalues by solving the Schrödinger equation in the framework of the NU method. We also calculate the NOR coefficient of GaAs/$Ga_{1-x}Al_xAs$ QDs under HPH confining potential. The calculation results indicate that the peak of NOR coefficient increases with the increasing T and V_3, but decreases with the increase of V_1, R_0, P, and V_2. In a specific Al-concentration range, the maximum value of NOR coefficient will decreases, meaning that we can obtain the required nonlinear optical properties by tuning Al-concentration. Furthermore, with the increasing T and V_3, the resonance peak of NOR coefficient appears in a red shift, but with the increasing V_1, R_0, P and V_2, the NOR coefficient appears in a blue shift. Also, the position of the peak has a blue shift as Al-concentration changes from 0.1 to 0.3. We think that the present results can play a guiding role in improving the nonlinear optical properties and optical modulation characteristics of low-dimensional semiconductor materials.

Acknowledgement

Project supported by the National Natural Science Foundation of China (Grant Nos. 51702003, 61775087, 11674312, 52174161, and 12174161).

References

[1] Noverola-Gamas H, Gaggero-Sager L M and Oubram O 2022 *Chin. Phys. B* **31** 044203
[2] Bejan D 2016 *Phys. Lett. A* **380** 3836
[3] Feng Z Y and Yan Z W 2016 *Chin. Phys. B* **25** 107804
[4] Li X C, Wang A M, Wang Z L and Yang Y 2012 *Chin. Phys. B* **21** 087303
[5] Liu C P and Hatsagortsyan K Z 2012 *Phys. Rev. A* **85** 023413
[6] Li X C, Ye C B, Gao J and Wang B 2020 *Chin. Phys. B* **29** 087302
[7] Yu Y B and Guo K X 2003 *Physica E* **18** 492
[8] Sun F L, Li Z H and Wei J H 2020 *Chin. Phys. B* **29** 067302
[9] Qin L G and Wang Q 2017 *Chin. Phys. Lett.* **34** 017303
[10] Duan Y M, Li X C, Chang C, Zhao Z and Zhang L C 2022 *Physica B* **631** 413644
[11] Zhang C J and Liu C P 2020 *Laser Phys. Lett.* **17** 085404
[12] Li J and Zhang D 2015 *Chin. Phys. Lett.* **32** 047303
[13] Pokutnyi S I 2020 *Eur. Phys. J. Plus* **135** 74
[14] Rezaei G, Vaseghi B, Khordad R and Kenary H A 2011 *Physica E* **43** 1853
[15] Yang J Y and Chen H J 2019 *Acta Phys. Sin.* **68** 246302 (in Chinese)
[16] Dapkus P D 1982 *Annu. Rev. Mater. Sci.* **12** 243
[17] Hersee S D and Duchemin J P 1982 *Annu. Rev. Mater. Sci.* **12** 65
[18] Hien N D, Duque C A and Feddi E 2019 *Thin Solid Films* **682** 10
[19] Zhang Z H, Guo K X, Chen B, Wang R Z, Kang M W and Shao S 2010 *Superlattices Microstruct.* **47** 325
[20] Zhang L C, Li X C, Liu X G and Li Z R 2021 *Physica B* **618** 413197
[21] Prasad V and Silotia P 2011 *Phys. Lett. A* **375** 3910
[22] Rezaei G, Vahdani M R K and Vaseghi B 2011 *Curr. Appl. Phys.* **11** 176
[23] Liu G H, Guo K X, Hassanabadi H and Lu L L 2012 *Physica B* **407** 3676
[24] Hou N, Du F Y, Feng R and Wu H S 2021 *J. Mol. Liq.* **331** 115720
[25] Liu K, Xu X, Shan W, Sun D, Yao C and Sun W 2020 *Opt. Mater.* **99** 109569
[26] Tung L V, Lam V T, Hoa L T and Phuc H V 2021 *Opt. Quantum Electron.* **53** 174
[27] Liu X, Zou L, Liu C, Zhang Z H and Yuan J H 2016 *Opt. Mater.* **53** 218
[28] Egrifes H and Sever R 2005 *Phys. Lett. A* **344** 117
[29] Máthé L, Onyenegecha C P, Farcaş A A, Pioraş-Ţimbolmaş L M, Solaimani M and Hassanabadi H 2021 *Phys. Lett. A* **397** 127262
[30] William E S, Inyang E P and Thompson E A 2020 *Rev. Mex. Fis.* **66** 730
[31] Greene R L and Aldrich C 1976 *Phys. Rev. A* **14** 2363
[32] Rezaei G, Vaseghi B, Khordad R and Kenary H A 2011 *Physica E* **43** 1853
[33] Yu Y B, Zhu S N and Guo K X 2005 *Phys. Lett. A* **335** 175